Journal of Sound and Vibration 329 (2010) 4705–4718

Contents lists available at ScienceDirect

Journal of Sound and Vibration

journal homepage: www.elsevier.com/locate/jsvi

On the interaction of sound with steady heat communicating flows

Nader Karimi [a], Michael J. Brear [b,*], William H. Moase [b]

[a] Institute of Reactive Flows and Diagnostics, Center of Smart Interfaces, Technical University of Darmstadt, Petersenstraße 32, 64287 Darmstadt, Germany
[b] Department of Mechanical Engineering, University of Melbourne, Parkville, 3010 Victoria, Australia

ARTICLE INFO

Article history:
Received 2 June 2009
Received in revised form
8 May 2010
Accepted 12 May 2010
Handling Editor: D. Juve
Available online 17 June 2010

ABSTRACT

This paper presents a theoretical and numerical investigation of the interaction between sound waves and non-diffusive, quasi-one-dimensional, subsonic flows with only steady heat communication. It is first shown that a steady heat communicating flow can attenuate or generate sound even in the absence of mean flow acceleration. The relative significance of sound generation by the heat addition induced acceleration of density or entropy inhomogeneities and the effect of steady heat communication on the incident acoustic wave is then found. It is shown through scaling arguments that at high frequencies mean flow acceleration effects are negligible and the only significant sound generating mechanism involves steady heat communication. At low frequencies, however, the two mechanisms are more comparable.

1. Introduction

Sound production in fluid flows with simultaneous heat communication and acceleration has important application in numerous engineering devices. These include rockets, gas turbines, heat exchangers and refrigerators, to name a few. In these cases, sound often coexists with unsteady heat addition or removal, as well as hydrodynamic and temperature fluctuations.

It has been known since Rayleigh [1] that unsteadiness in the communication of heat to or from a flow can generate or attenuate sound. Ffowcs Williams and Howe [2] and Howe [3,4] also showed that the acceleration of density and entropy inhomogeneities can be a sound source. As heat communicating flows are normally accelerating or decelerating, these mechanisms are sometimes considered to be the main sound generating mechanisms in combusting flows [5–9]. There are other sources of noise in combusting flows, such as those rising from viscous and diffusion effects [10,11], chemical inhomogeneities [12] and flame front interactions [6].

Recently, Karimi et al. [13] considered a non-reacting, inviscid and non-heat conducting flow, and showed theoretically and numerically that steady heat communication can generate sound. However, the origin of this sound generation was not clear since their test cases included flows with both steady heat communication and steady flow acceleration. It is well known that the interaction of sound with heat communicating flows can generate entropy disturbances [13–17]. Following Howe [3], these disturbances can then generate sound as they are convected by the accelerating mean flow due to the mean temperature gradient. Therefore, the sound generation in studies such as Karimi et al. [13] can either be by the acceleration of these entropic disturbances or potentially involve additional sources.

Two duct flows are considered in this paper (Fig. 1). In each group both flows have identical upstream mean Mach number $\overline{M}_0$, static temperature $\overline{\theta}_0$ and pressure $\overline{p}_0$. Two homogeneous, semi-infinite regions are located upstream and

* Corresponding author. Tel.: +61 3 8344 6722; fax: +61 3 8344 4290.
E-mail address: mjbrear@unimelb.edu.au (M.J. Brear).

0022-460X/$ - see front matter © 2010 Published by Elsevier Ltd.
doi:10.1016/j.jsv.2010.05.009

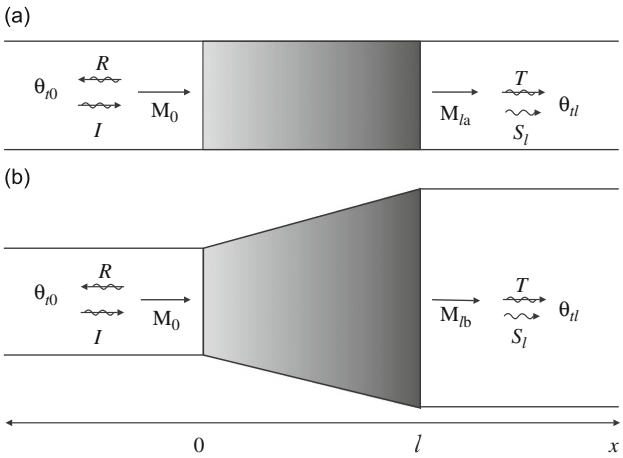

Fig. 1. Schematic of the heating configuration, (a) one-dimensional accelerating flow, (b) quasi-one-dimensional non-accelerating flow, l=1 m, $\theta_{t0}=600$ K, $\theta_{tl}=1200$ or 1800 K where θ_t is the stagnation temperature, unless stated otherwise.

downstream of a region of steady heat communication, which have constant cross-sectional areas. The steady heat communication is through external means and results in a linear increase or decrease in the mean stagnation temperature from $\overline{\theta}_{t_0}$ at x=0 to $\overline{\theta}_{t_l}$ at x=l. Thus, the mean heat communication to the two flows is the same. In all cases studied throughout this paper the unsteadiness in heat communication is zero. Further, as will be detailed in Section 3.1, the cross-sectional area in Fig. 1b changes in such a way that the mean flow does not accelerate. The system is excited by a downstream travelling acoustic wave I and the response is characterised by the reflected R and transmitted T acoustic waves as well as an outgoing entropy disturbance S_l. These acoustic disturbances are given by

$$p'(t,0)=\mathrm{Re}[\exp(\mathrm{i}\omega t)(I+R)],$$

$$u'(t,0)=\mathrm{Re}[\exp(\mathrm{i}\omega t)(I-R)1/\overline{\rho}_0\overline{c}_0],$$

and

$$p'(t,l)=\mathrm{Re}[\exp(\mathrm{i}\omega t)(T\exp(-\mathrm{i}\omega l/c))],$$

where Re symbol indicates the real part.

In these equations the terms p (Pa), ρ (kg/m^3), c (m/s), ω (rad/s) and u (m/s) are respectively the static pressure, static density, isentropic sound speed, frequency and flow velocity. In general any given property g may be split into a steady $\overline{g}$ and disturbance quantity g' such that $g=\overline{g}+g'$. Unless otherwise stated, throughout this paper the inlet and exhaust stagnation temperature and length of the inhomogeneous region (l) are those specified in Fig. 1. Further, the configurations in Fig. 1a and b are referred to as cases A and B respectively.

It should be noted that the flows shown in Fig. 1 are not intended to be closely representative of real flows. In particular, the flow within a gas turbine combustor features unsteady heat release, strong turbulence and non-equilibrium chemistry, to name a few. None of these are considered in this paper. In particular, unsteady heat release is a well-known and significant sound source in combustion [5,6]. The relative magnitude of sound generation by steady versus unsteady heat addition depends on the relative magnitude of the mean and unsteady sources, which is not the subject of this paper. Rather, sound sources due only to steady heat communication and the acceleration that it can induce are examined over temperature ratios that are representative of some devices.

2. Theoretical and numerical methods

2.1. Theory

2.1.1. Equations of motion

Consider the quasi-one-dimensional Euler equations applied to a calorifically perfect and ideal gas

$$\frac{\partial}{\partial t}(\rho A)+\frac{\partial}{\partial x}(\rho uA)=0, \tag{1}$$

$$\frac{\partial}{\partial t}(\rho uA)+\frac{\partial}{\partial x}([p+\rho u^2]A)=p\frac{\mathrm{d}A}{\mathrm{d}x}, \tag{2}$$

$$\frac{\partial}{\partial t}\left(\left[\frac{p}{\gamma-1}+\frac{1}{2}\rho u^2\right]A\right)+\frac{\partial}{\partial x}\left(\left[\frac{\gamma p}{\gamma-1}+\frac{1}{2}\rho u^2\right]uA\right)=Q, \tag{3}$$

where Q (W/m) is the heat communication per unit length and $\gamma=1.4$ throughout this paper. The terms q (W/m^3), γ, c_p (J/kg K), s (J/kg K), and A (m^2) are respectively the heat communication per unit volume, specific heat ratio, specific heat capacity, entropy and the cross-sectional area.

It is important to note that although diffusive heat transfer has been neglected in the present problem, heat addition or subtraction can still be achieved by heat communication through an external means. This is a reasonable approximation for a reacting flow in the equilibrium chemistry limit and also for incident or emitted radiation.

2.1.2. Acoustic energy

The analysis presented in this paper is linear. It should be noted that in real flows interaction of flames with acoustics can involve strong nonlinearity [18,19], but this usually appears in the flame dynamics rather than the acoustics. Consider the acoustic energy balance for quasi-one-dimensional, non-diffusive, heat communicating flows derived by Bloxsidge et al. [20], which extends Morfey's earlier work [21]:

$$\frac{\partial}{\partial t}(eA)+\frac{\partial}{\partial x}(EA)=D, \tag{4}$$

where

$$e=p'^2/2\overline{\rho}\overline{c}^2+\overline{\rho}u'^2/2+\overline{u}p'u'/\overline{c}^2 \tag{5}$$

is the acoustic energy density (J/m^3) and

$$E=p'u'+\overline{\rho}\overline{u}u'^2+\overline{u}^2p'u'/\overline{c}^2+\overline{u}p'^2/\overline{\rho}\overline{c}^2 \tag{6}$$

is the acoustic energy flux (W/m^2). Bloxsidge et al. [20] expressed the acoustic energy source term D (W/m) as

$$D=(\overline{\rho}\overline{u}u'+p')\frac{\overline{q}A(\gamma-1)}{\gamma\overline{p}}\left(\frac{q'}{\overline{q}}-\frac{p'}{\overline{p}}-\frac{u'}{\overline{u}}\right)+\left(u'+\frac{\overline{u}p'}{\overline{\rho}\overline{c}^2}\right)A\left[\left(\frac{\overline{\rho}s'}{c_p}-\frac{p'}{\overline{c}^2}\right)\overline{u}\frac{\mathrm{d}\overline{u}}{\mathrm{d}x}-\frac{p'}{\overline{\rho}}\frac{\mathrm{d}\overline{\rho}}{\mathrm{d}x}\right]. \tag{7}$$

Eqs. (1)–(3) can be combined to give

$$\overline{u}\left(\frac{\overline{u}}{\overline{c}^2}\frac{\mathrm{d}\overline{u}}{\mathrm{d}x}+\frac{1}{\overline{\rho}}\frac{\mathrm{d}\overline{\rho}}{\mathrm{d}x}\right)=\frac{\gamma-1}{\gamma}\frac{\overline{q}}{\overline{p}}. \tag{8}$$

Thus, Eq. (7) can be rearranged in the following way:

$$D=D_{\mathrm{uhc}}+D_{\mathrm{shc}}+D_{\mathrm{mfa}}, \tag{9}$$

where

$$D_{\mathrm{uhc}}=\frac{\overline{q}A(\gamma-1)}{\gamma\overline{p}}(\overline{\rho}\overline{u}u'+p')\frac{q'}{\overline{q}}, \tag{10}$$

$$D_{\mathrm{shc}}=-\frac{\overline{q}A(\gamma-1)}{\gamma\overline{p}}\left[(\overline{\rho}\overline{u}u'+p')\left(\frac{p'}{\overline{p}}+\frac{u'}{\overline{u}}\right)-p'\left(\frac{u'}{\overline{u}}+\frac{p'}{\overline{\rho}\overline{c}^2}\right)\right], \tag{11}$$

$$D_{\mathrm{mfa}}=A\overline{u}\frac{\mathrm{d}\overline{u}}{\mathrm{d}x}\left(u'+\frac{\overline{u}p'}{\overline{\rho}\overline{c}^2}\right)\frac{\overline{\rho}s'}{c_p} \tag{12}$$

are respectively the source terms due to unsteady heat communication, steady heat communication and mean flow acceleration. An alternative arrangement of source terms in terms of density disturbances is put forward in Appendix C.

With the arrangement in Eqs. (9)–(12) we consider two mechanisms which can generate sound in the absence of unsteady heat communication (i.e. D_{uhc}=0). First D_{mfa} describes sound generation by the acceleration of entropy disturbances. The remaining terms then only depend on the steady heat communication and so are grouped as D_{shc}. It is not clear how significant D_{shc} is compared to the well-established mechanism of acceleration of entropy inhomogeneities [3].

Eqs. (4)–(6) and (9) are applied over the inhomogeneous region in Fig. 1. The flux term in these equations was first derived by Cantrell and Hart [22] for acoustic propagation in a moving medium with homogeneous mean flow. It is therefore a well posed, acoustic flux in the upstream and downstream homogeneous regions, where acoustic and entropic disturbances are decoupled [17]. Sound production within the inhomogeneous region can then be determined by examining the balance of these acoustic fluxes in the homogeneous regions,

$$\overline{E_lA_l}-\overline{E_0A_0}=\int_0^l\overline{D}\,\mathrm{d}x. \tag{13}$$

The integral of $\overline{D}$ over the inhomogeneous region can then be considered to be purely acoustic even though D at any point within the inhomogeneous region may not be purely acoustic.

2.2. Numerical solver

The present work solves Eqs. (1)–(3) in conservation form by using the dispersion-relation-preserving (DRP) scheme of Tam and Webb [23]. The specific DRP scheme chosen uses an optimised, four level, time marching scheme and seven point stencil for spatial differentiation. The choice of such a scheme ensures that the computed waves are a good approximation of the exact Euler equations. Non-reflecting boundary conditions are implemented to ensure that the numerical domain approximates an infinite domain. The exact boundary conditions follow the same formulation given by Poinsot and Lele [24] to ensure that the incoming waves at each boundary are always zero. An exception to this is in the implementation of the system excitation. The system can be forced by an incoming downstream travelling pressure or entropy wave at the inlet. The amplitude of the system excitation is small enough to ensure that the system is always linear. Numerical damping is employed to remove non-physical high-frequency waves from the solution. This is a modified version of the scheme of Tam and Shen [25], and incorporates damping in regions of entropy discontinuity. All simulations are run with a Courant–Friedrichs–Lewy number of 0.1. The number of grid points in the inhomogeneous region used in each simulation is 601. Simulations are run for a sufficiently long time to ensure that no transients are present in the final results. This solver has been validated on several problems, such as those presented by the authors in [13,26], as well as on the results presented in this paper.

3. Results and discussion

3.1. Zero and low mean flow velocity

The cross-sectional area variation for the non-accelerating mean flow, case B, is found from the equations of motion. It follows from Eqs. (1) and (2) that for a quasi-one-dimensional, constant mean velocity flow the mean pressure must remain constant. The equation of state for an ideal gas then requires that $\overline{\theta}\,\mathrm{d}\overline{\theta}/\mathrm{d}x=-\overline{\rho}\,\mathrm{d}\overline{\rho}/\mathrm{d}x$, which upon substitution into Eq. (1) results in

$$\frac{1}{\overline{A}}\frac{\mathrm{d}A}{\mathrm{d}x}=\frac{1}{\overline{\theta}}\frac{\mathrm{d}\overline{\theta}}{\mathrm{d}x}. \tag{14}$$

Here, $\overline{\theta}_t(x)=\overline{\theta}_{t_0}+mx$ in which m (K/m) is a constant, is considered along the inhomogeneous region. Noting that $\overline{\theta}_t=\overline{\theta}+\overline{u}^2/2C_p$ and $\overline{u}$ is constant in case B, Eq. (14) can be integrated to give

$$\frac{A(x)}{A_0}=\frac{\overline{\theta}_0+mx}{\overline{\theta}_0},\quad 0\le x\le l. \tag{15}$$

The zero mean flow case is first considered. In this case the mean heat communication must be also zero and thus, the temperature distribution becomes an initial condition for this non-diffusive flow. Eq. (4) then reduces to the classical acoustic energy equation [27]. As required by the first law of thermodynamics, the net average classical acoustic energy fluxes entering and leaving the region with mean temperature gradient must be the same [13,28] and therefore

$$\frac{A_l}{A_0}\frac{\overline{\rho}_0\overline{c}_0}{\overline{\rho}_l\overline{c}_l}\left(\frac{T}{I}\right)^2+\left(\frac{R}{I}\right)^2=1. \tag{16}$$

Hence, the acoustic energy reflection and transmission coefficients for zero Mach number are defined as $\Sigma_R=(R/I)^2$ and $\Sigma_T=(A_l/A_0)(\overline{\rho}_0\overline{c}_0/\overline{\rho}_l\overline{c}_l)(T/I)^2$ respectively. Fig. 2 shows the analytically calculated frequency response of these coefficients for this zero mean flow condition for cases A and B. The details of the derivation for the varying cross-sectional area flow are in Appendix A, while that for constant cross-sectional flow has been presented by Karimi et al. [13].

Introduction of mean flow results in non-zero mean heat communication and also generation of entropy [13,15,17]. The acoustic energy reflection and transmission coefficients are now defined using the flux term of Eq. (4) and take the form

$$\Sigma_R=\frac{(1-\overline{M}_0)^2}{(1+\overline{M}_0)^2}\left|\frac{R}{I}\right|^2,\quad \Sigma_T=\frac{A_l}{A_0}\frac{\overline{\rho}_0\overline{c}_0}{\overline{\rho}_l\overline{c}_l}\frac{(1+\overline{M}_l)^2}{(1+\overline{M}_0)^2}\left|\frac{T}{I}\right|^2. \tag{17}$$

Fig. 2 also shows the numerically calculated values of the reflection and transmission coefficients for an inlet Mach number of 0.01. As can be seen, there is a good agreement between the low Mach number numerical simulations and analytically calculated coefficients for zero mean flow. As perhaps expected, the amplitude of the acoustic energy reflection coefficient is generally higher for the flow with varying cross-sectional area, since in this flow the mean temperature gradient and the change in the flow cross-sectional area are both responsible for the sound reflection. Further, the phase of the reflection and transmission coefficients for the cases A and B are identical at zero mean flow. This is because, in the absence of mean flow, the phases of the reflection and transmission coefficients are determined by the adiabatic sound speed which is the same in the two cases at a given axial position.

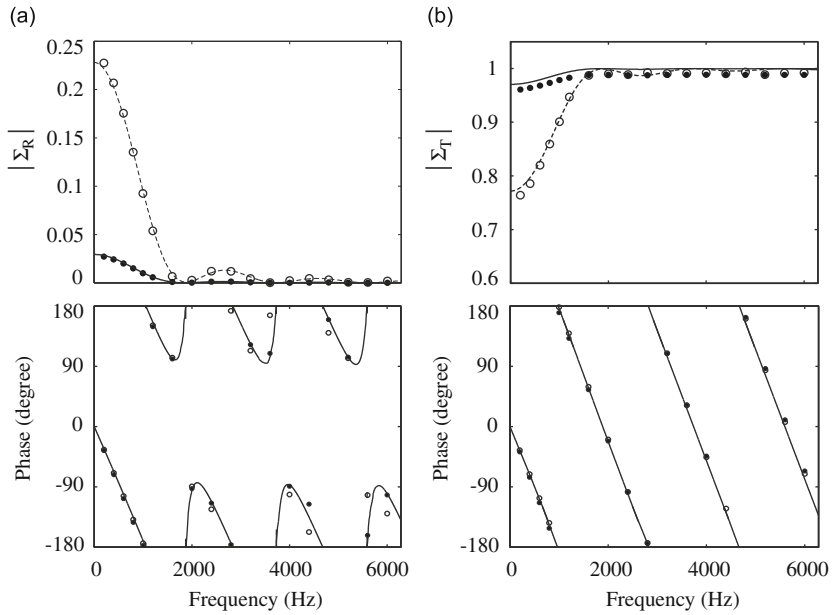

Fig. 2. Amplitude and phase of the acoustic energy (a) reflection and (b) transmission coefficients. Solid lines (zero mean flow analytical result) and dots (simulations for $\overline{M}_0 = 0.01$) for case A. Dashed lines (zero mean flow analytical result) and circles (simulations for $\overline{M}_0 = 0.01$) for case B.

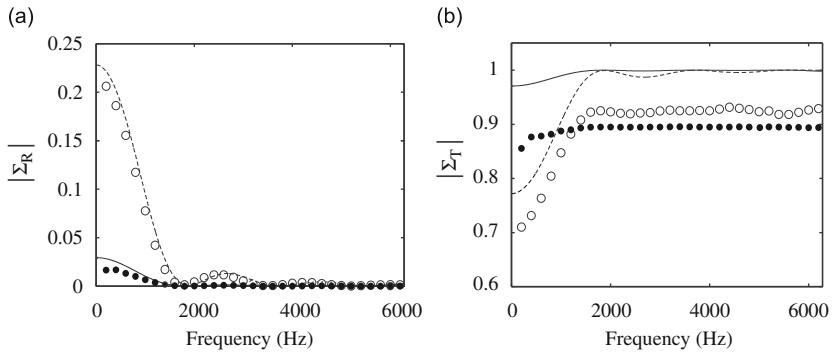

Fig. 3. Amplitude of the acoustic energy (a) reflection and (b) transmission coefficients. Solid lines (zero mean flow analytical result) and dots (simulations for $\overline{M}_0 = 0.1$) case A. Dashed lines (zero mean flow analytical result) and circles (simulations for $\overline{M}_0 = 0.1$) for case B.

3.2. Higher mean flow velocities

Increasing the inlet mean flow Mach number to 0.1 results in considerable sound attenuation in both cases A and B (Fig. 3). This attenuation occurs for all forcing frequencies and is similar for the two cases.

The attenuation of sound for finite mean velocities can be also studied analytically at low forcing frequencies, in which the heat communicating region can be considered acoustically compact (Appendix B). Fig. 4 shows the analytic compact analyses for cases A and B and heated flows, with two different stagnation temperature ratios. Here, the sum of the amplitudes of the acoustic energy reflection and transmission coefficients shows the fraction of the total incident acoustic energy which has been dissipated in the heat communicating region. As can be seen, this sound attenuation increases for the non-accelerating flow as the inlet Mach number increases, although in the accelerating flow the attenuation is more pronounced. At sufficiently high $\overline{M}_0$, thermal choking of the accelerating flow occurs ($\overline{M}_0 = 0.38$ and 0.29 for stagnation temperature ratios of 2 and 3 respectively).

Fig. 5 shows the compact analytic analyses for two cooled flows. The case B flow now contracts. The flow cannot of course choke, and overall sound production is now observed in both cases. Figs. 4 and 5 also include numerical results for simulation at low forcing frequency (100 rad/s in these cases), which are in very good agreement with the analytical compact results.

Fig. 6 extends this analysis numerically to higher forcing frequencies. This figure shows that both flows in cases A and B attenuate sound by steady heating to a comparable extent for almost all forcing frequencies and inlet Mach numbers.

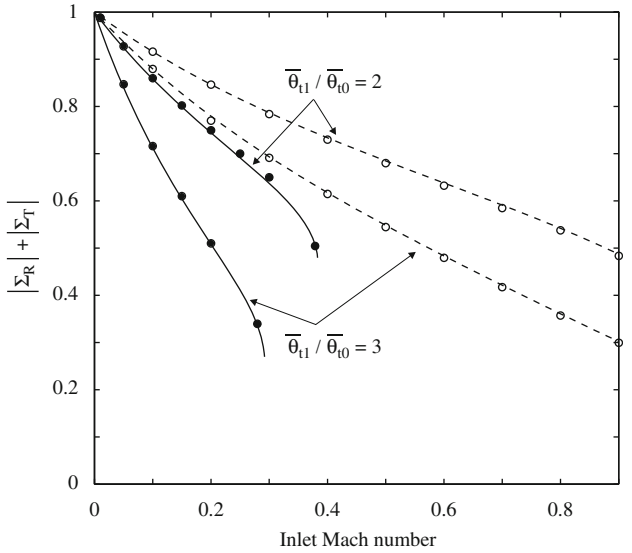

Fig. 4. Sum of the amplitudes of the acoustic energy reflection and transmission coefficients for the heated flows. Solid lines (compact analytical results) and dots (simulation) for case A. Dashed lines (compact analytical results) and circles (simulation) for the case B.

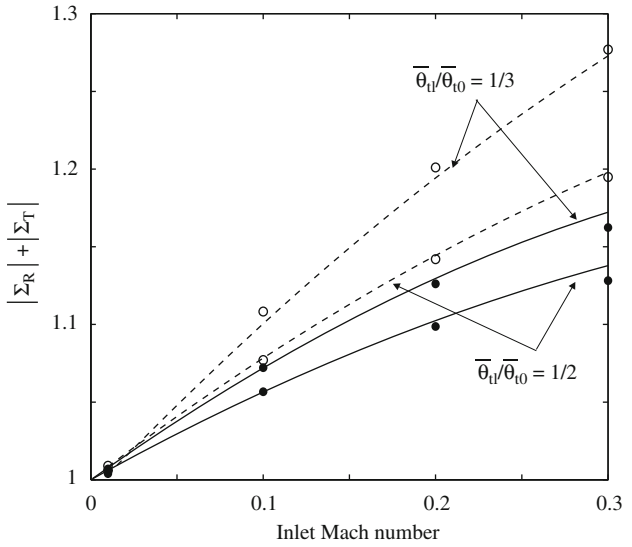

Fig. 5. Sum of the amplitudes of the acoustic energy reflection and transmission coefficients for cooled flows. Solid lines (compact analytical results) and dots (simulation) for case A. Dashed lines (compact analytical results) and circles (simulation) for the case B.

However, at higher inlet Mach numbers and low frequency the accelerating flow shows more attenuation compared to that at the same inlet Mach number and higher frequency. This is due to stronger generation of entropy disturbances at low frequencies, and will be further investigated in the following section.

3.3. High and low frequency asymptotic behaviour

Karimi et al. [13] showed that when $\lambda_c/l \ll 1$ (where λ_c is the convective wavelength) and under acoustic excitation there are negligible entropy disturbances in any steady heat communicating flow. It follows that in this limit $D_{\mathrm{mfa}} \to 0$ and the *only* existing sound generating mechanism is that by steady heat communication D_{shc}.

At the limit of zero frequency the generation of entropy is significant [13]. Thus, D_{mfa} is expected to be large at this limit. To compare the relative significance of D_{mfa} and D_{shc} at low frequencies a new parameter Ω is defined:

$$\Omega = 1/l \int_0^l \overline{D_{\mathrm{shc}}}/\overline{D_{\mathrm{mfa}}}\, \mathrm{d}x. \tag{18}$$

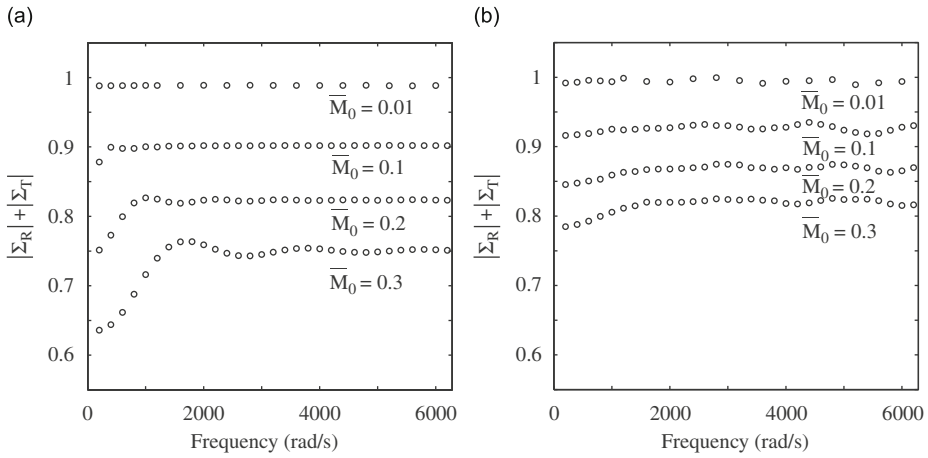

Fig. 6. Sum of amplitudes of the acoustic energy reflection and transmission coefficients at varying inlet mean Mach number, (a) accelerating flow (case A), (b) non-accelerating flow (case B).

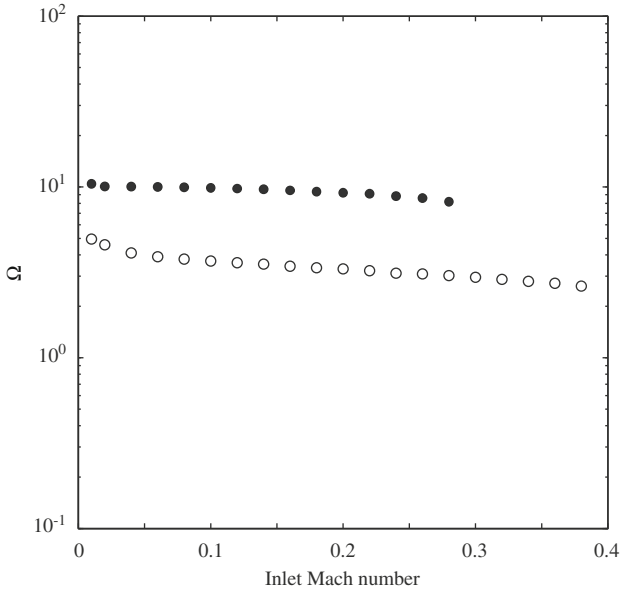

Fig. 7. Calculated value of Ω for stagnation temperature ratios of 2 (circles) and 3 (dots) for case A at low frequency.

Fig. 7 shows the values of Ω in case A calculated for a range of inlet Mach numbers and varying excitation frequencies such that $\lambda_c/l = 2$ always, where λ_c is based on the average mean flow velocity along the heat communicating region. At low frequencies, the term D_{shc} is of the same order but stronger than D_{mfa}, with the former becoming more dominant as the temperature ratio increases.

These arguments are consistent with the trend observed in Fig. 6. Consider for example $\overline{M}_0 = 0.1$ at the highest frequency shown in this figure, $\lambda_c/l \simeq 0.06$, and the total acoustic energy flux attenuation of the accelerating and non-accelerating flows are very similar. The small difference between the two is due to different steady mean velocity and pressure distributions in the two flows, which become more significant as the inlet Mach number increases. However, at low frequency the accelerating flow shows more attenuation. Once again, this attenuation increases with inlet Mach number and is due to acceleration of entropy disturbances at high Mach numbers as shown in Fig. 7.

3.4. Entropic forcing of case B flow

The rest of this paper is concerned with entropic excitation of the inhomogeneous region. Entropic excitation of the inhomogeneous region can also generate sound for the case A flow, as shown by the authors in some detail in an earlier

work [13]. This section shows analytically that there can be no sound generation by the inhomogeneous region for case B flow and forcing by incident, convective, entropy disturbances.

Consider the equations of conservation of mass, momentum and energy (Eqs. (1)–(3)). Combining the equations of mass and momentum reveals

$$\frac{\partial u}{\partial t}+\frac{1}{\rho}\frac{\partial p}{\partial x}+u\frac{\partial u}{\partial x}=0, \tag{19}$$

and equations of mass, momentum and energy can be rearranged to give

$$\frac{\partial p}{\partial t}-(\gamma-1)u\frac{\partial p}{\partial x}+\frac{\gamma}{A}\frac{\partial(puA)}{\partial x}=\frac{(\gamma-1)Q}{A}. \tag{20}$$

Now, for case B flow $\mathrm{d}\overline{u}/\mathrm{d}x=0$ everywhere. Linearising Eqs. (19) and (20) for non-accelerating flows then results in respectively

$$\frac{\partial u'}{\partial t}+\frac{1}{\overline{\rho}}\frac{\partial p'}{\partial x}+\overline{u}\frac{\partial u'}{\partial x}=0, \tag{21}$$

$$\frac{\partial p'}{\partial t}=-\overline{u}\frac{\partial p'}{\partial x}-\frac{\gamma}{A}\frac{\mathrm{d}A}{\mathrm{d}x}(\overline{p}u'+\overline{u}p')-\gamma\overline{p}\frac{\partial u'}{\partial x}+\frac{(\gamma-1)Q}{A}. \tag{22}$$

Eqs. (21) and (22) only rely on p', u' and mean flow properties. Therefore, the solution of these equations which reveals the acoustic field in the homogeneous regions is independent of incident density or entropy disturbances. Thus, incident entropic forcing of case B flow cannot result in sound generation. Numerical simulations confirm this.

4. Conclusions

The generation of sound due to the interaction of incident acoustics and entropic disturbances with steady heat communication was studied numerically and theoretically. Two sets of flows were considered with identical upstream conditions and steady heat addition or heat removal. One of these flows was one-dimensional, and therefore accelerating, whilst the other featured a varying cross-sectional area such that the mean flow velocity was constant. The numerical simulation of these two flows was validated against the analytical results for zero mean flow and also compact non-zero mean flow results.

It was first observed that incident acoustic energy was dissipated by both the accelerating and non-accelerating flows with mean heat addition. The extent of this attenuation was more pronounced for the accelerating flow, but attenuation in both cases was of the same order of magnitude and increased as the inlet Mach number increased. Conversely, mean heat removal generated sound, and numerical solutions again agreed with the theory presented.

Asymptotic arguments showed that the generation of entropy disturbances were negligible at high frequencies and therefore sound generation due to the acceleration of entropy disturbances approached zero. Thus, in this limit, the generation/attenuation of sound in either of the accelerating and non-accelerating flows was exclusively through steady heat communication.

Considering then the acceleration of either entropy or density disturbances, scaling analysis revealed that at high frequencies and low Mach numbers the mean flow acceleration effect is weak compared to that by steady heat communication. At low frequencies, however, the two sound generating mechanisms were observed to be more comparable.

Acknowledgement

The authors would like to thank Prof. Nigel Peake of the University of Cambridge for thoughtful discussions on earlier drafts of this work.

Appendix A. Frequency response of a region with mean temperature gradient, varying cross-sectional and zero mean flow

This section derives an analytical solution for the reflection and transmission of acoustic energy from a region with zero mean flow, finite mean temperature gradient and varying cross-sectional area, satisfying Eq. (14). This builds heavily on the work of Subrahmanyam and Sujith [29] and extends the approach presented in [13].

Subrahmanyam and Sujith [29] considered an inhomogeneous non-uniform duct with zero mean velocity and a known relationship between the mean temperature and the duct cross-sectional area. They assumed harmonic solutions of the form $p'(x,t)=P'(x)\exp(\mathrm{i}\omega t)$, and expressed the acoustic wave equation as

$$\frac{\mathrm{d}^2P'}{\mathrm{d}x^2}+\left[\frac{1}{A}\frac{\mathrm{d}A}{\mathrm{d}x}+\frac{1}{\overline{\theta}}\frac{\mathrm{d}\overline{\theta}}{\mathrm{d}x}\right]\frac{\partial P'}{\partial x}-\frac{\omega^2}{\gamma R\overline{\theta}}P'=0. \tag{A.1}$$

To solve Eq. (A.1) the following transformation was introduced

$$\zeta = \int \frac{\mathrm{d}x}{A\overline{\theta}}. \tag{A.2}$$

Now consider the temperature and cross-sectional area distribution discussed in Section 3.1,

$$\overline{\theta} = \overline{\theta}_0 + mx, \quad A = h(\overline{\theta}_0 + mx), \tag{A.3}$$

where h (m^2/K) is A_0/θ_0. Upon substitution of A and θ from (A.3), relation (A.2) becomes

$$\zeta = \frac{-1}{mh}\frac{1}{(\overline{\theta}_0 + mx)}. \tag{A.4}$$

Eq. (A.1) can be rewritten as

$$\frac{\mathrm{d}^2P'}{\mathrm{d}\zeta^2} + (\kappa A^2\overline{\theta})P' = 0, \tag{A.5}$$

where $\kappa = \omega^2/(\gamma R)$. New parameters a and κ^* are considered such that

$$A^2\overline{\theta} = (a\kappa^*\zeta)^n, \tag{A.6}$$

where $\kappa^* = (\kappa)^{-1/n}$ and for the present problem $n = -3$, $\kappa^* = (\gamma R/\omega^2)^{-1/3}$ and $a = -(\gamma R h m^3/\omega^2)^{1/3}$. Eq. (A.1) transforms into

$$\frac{\mathrm{d}^2P'}{\mathrm{d}\zeta^2} + (a\zeta)^n P' = 0. \tag{A.7}$$

Subrahmanyam and Sujith [29] introduced new variables as follows:

$$r = (a\kappa^*\zeta)^{1/2\nu}, \quad P' = r^\nu z, \tag{A.8}$$

where $\nu = 1/(n+2)$. Substituting from Eqs. (A.2) and (A.6) into Eq. (A.8) results in

$$r = h^{1/3}(\theta_0 + mx)^{1/2}, \quad \nu = -1. \tag{A.9}$$

Substituting variables from Eqs. (A.8) and (A.9), reduces (A.7) into a standard Bessel's differential equation

$$\frac{\mathrm{d}^2z}{\mathrm{d}r^2} + \frac{1}{r}\frac{\mathrm{d}z}{\mathrm{d}r} + \left[\alpha^2\kappa - \frac{\nu^2}{r^2}\right]z = 0, \tag{A.10}$$

where $\alpha = 2\nu/(a\kappa^*) = 2/(m^3 \cdot h)^{1/3}$. General solutions of the pressure and velocity disturbances are then

$$P' = s^\nu[c_1 J_\nu(\beta r) + c_2 Y_\nu(\beta r)], \tag{A.11}$$

$$U' = \frac{\mathrm{i}}{\rho\omega}\frac{\mathrm{d}r}{\mathrm{d}x} r^\nu \left\{\frac{\nu}{r}(c_1 J_\nu(\beta r) + c_2 Y_\nu(\beta r)) + \frac{\beta}{2}[c_1(J_{\nu-1}(\beta r) - J_{\nu+1}(\beta r)) + c_2(Y_{\nu-1}(\beta r) - Y_{1+\nu}(\beta r))]\right\}, \tag{A.12}$$

where $\beta^2 = \alpha^2\kappa$. The boundary conditions which specify c_1 and c_2 are derived from the configuration of the problem. The incident acoustic wave I in Fig. 1 has a velocity fluctuation such that $U'(0) = \varepsilon$, where ε is a constant. Further, Karimi et al. [13] showed that the anechoic boundary condition for the cases such as the present configuration takes the form

$$P'(l) = \overline{\rho}_l \overline{c}_l U'(l). \tag{A.13}$$

Eqs. (A.11) and (A.12) then allow determination of the constants c_1 and c_2,

$$c_2 = \frac{EH}{GH - KF}, \quad c_1 = \frac{EK}{FK - HG}, \tag{A.14}$$

where

$$F = \frac{-J_{-1}(\beta r(0))}{r(0)} + \frac{\beta}{2}[J_{-2}(\beta r(0)) - J_0(\beta r(0))], \tag{A.15}$$

$$G = \frac{-Y_{-1}(\beta r(0))}{r(0)} + \frac{\beta}{2}[Y_{-2}(\beta r(0)) - Y_0(\beta r(0))], \tag{A.16}$$

$$E = -\frac{\mathrm{i}\varepsilon r(0)\overline{\rho}_0\omega}{\mathrm{d}r(0)/\mathrm{d}x}, \tag{A.17}$$

$$H = J_{-1}(\beta r(l)) + \frac{\overline{c}_l}{\omega}\frac{\mathrm{d}r(l)}{\mathrm{d}x}\frac{\mathrm{i}J_{-1}(\beta r(l))}{r(l)} - \frac{\mathrm{i}\overline{c}_l}{\omega}\frac{\mathrm{d}r(l)}{\mathrm{d}x}\frac{\beta}{2}[J_{-2}(\beta r(l)) - J_0(\beta r(l))], \tag{A.18}$$

$$K = Y_{-1}(\beta r(l)) + \frac{\overline{c}_l}{\omega}\frac{\mathrm{d}r(l)}{\mathrm{d}x}\frac{\mathrm{i}Y_{-1}(\beta r(l))}{r(l)} - \frac{\mathrm{i}\overline{c}_l}{\omega}\frac{\mathrm{d}r(l)}{\mathrm{d}x}\frac{\beta}{2}[Y_{-2}(\beta r(l)) - Y_0(\beta r(l))]. \tag{A.19}$$

A.1. Reflection and transmission coefficients

Considering the upstream and downstream homogeneous regions and the relations between pressure, velocity and I, R and T, it follows that

$$\left|\frac{R}{I}\right| = \left|\frac{P'(0) - \overline{\rho}_0\overline{c}_0U'(0)}{P'(0) + \overline{\rho}_0\overline{c}_0U'(0)}\right|, \tag{A.20}$$

$$\left|\frac{T}{I}\right| = \left|\frac{P'(l)}{P'(0) + \overline{\rho}_0\overline{c}_0U'(0)}\right|. \tag{A.21}$$

Eqs. (A.14), (A.11) and (A.12) can then be used to calculate the reflection and transmission coefficients analytically.

Appendix B. Compact analysis of a region with non-zero mean flow

In this appendix, analytical expressions are derived for the reflection and transmission coefficients expressed in Eq. (17) through application of the linearised equations of mass, momentum and energy to a compact inhomogeneous region in case B. The equivalent analysis for the configuration shown in case A has been presented in Karimi et al. [13].

B.1. Momentum equation for a compact region with area change and constant mean velocity

Care must be taken when applying the momentum equation to a flow with area change in the compact limit. This section derives the appropriate jump condition for a subsonic nozzle or diffuser with zero mean flow acceleration as detailed in Section 3.1.

The quasi-one-dimensional linearised momentum equation is

$$\frac{\partial}{\partial x}[p'A + (\rho uA)'\overline{u} + (\overline{\rho u}A)u'] = p'\frac{\mathrm{d}A}{\mathrm{d}x}. \tag{B.1}$$

Considering the conditions of fixed mean flow velocity discussed in Section 3.1, Eq. (B.1) can be simplified to

$$\frac{\partial}{\partial x}\left(\frac{p'}{\overline{p}}\right) + \gamma\overline{M}^2\frac{\partial}{\partial x}\left(\frac{u'}{\overline{u}}\right) = 0. \tag{B.2}$$

The quasi-one-dimensional, equations of conservation of mass and energy can be combined to give

$$\frac{\partial}{\partial x}\left[\frac{1}{\overline{M}^2}\frac{u'}{\overline{u}} + \frac{1}{\overline{M}^2}\frac{p'}{\overline{p}} + (\gamma-1)\frac{u'}{\overline{u}}\right] = 0. \tag{B.3}$$

Combining Eq. (B.3) with (B.1) reveals

$$\frac{p'}{\overline{p}} = \overline{M}^4\left(\frac{\mathrm{d}\overline{M}^2}{\mathrm{d}x}\right)^{-1}\frac{\partial}{\partial x}\left[\frac{u'}{\overline{u}}\left(\frac{1-\overline{M}^2}{\overline{M}^2}\right)\right]. \tag{B.4}$$

Substituting Eq. (B.4) into Eq. (B.1) results in

$$\gamma\overline{M}^2\frac{\partial}{\partial x}\left(\frac{u'}{\overline{u}}\right) + \frac{\partial}{\partial x}\left[\overline{M}^4\left(\frac{\mathrm{d}\overline{M}^2}{\mathrm{d}x}\right)^{-1}\frac{\partial}{\partial x}\left[\frac{u'}{\overline{u}}\left(\frac{1-\overline{M}^2}{\overline{M}^2}\right)\right]\right] = 0. \tag{B.5}$$

Eq. (B.5) can be now simplified and solved for $(u'/\overline{u})$, which after some algebra, reduces to

$$\frac{\partial}{\partial x}\left(\frac{u'}{\overline{u}}\right) = Z\frac{\mathrm{d}}{\mathrm{d}x}[(1-\overline{M}^2)^{\gamma-1}], \tag{B.6}$$

where Z is a constant. Substituting for $(u'/\overline{u})$ from Eq. (B.6) into the momentum equation and solving, results in

$$\frac{(p'_l - p'_0)}{\overline{p}} = Z\Big[(\gamma-1)[(1-\overline{M}_l^2)^{\gamma} - (1-\overline{M}_0^2)^{\gamma}]^{\gamma} - \gamma[(1-\overline{M}_l^2)^{\gamma-1} - (1-\overline{M}_0^2)^{\gamma-1}]\Big]. \tag{B.7}$$

Finally, substituting for Z from (B.6) reveals the jump condition as

$$\frac{(p'_l - p'_0)}{\gamma\overline{p}} + \frac{(u'_l - u'_0)}{\overline{u}} = \left(\frac{u'_l - u'_0}{\overline{u}}\right)\left(\frac{\gamma-1}{\gamma}\right)\left[\frac{(1-\overline{M}_l^2)^{\gamma} - (1-\overline{M}_0^2)^{\gamma}}{(1-\overline{M}_l^2)^{\gamma-1} - (1-\overline{M}_0^2)^{\gamma-1}}\right]. \tag{B.8}$$

B.2. Reflection and transmission coefficients

Application of Eq. (B.8) and mass and energy conservation to a compact region with mean temperature and cross-sectional area jump results in the following reflection and transmission coefficients:

$$\frac{R}{I}=\frac{\Gamma\Upsilon(A_0/A_l)+\Theta\Lambda}{\Lambda\Xi-\Gamma\Pi(A_0/A_l)},\quad \frac{T}{I}=\frac{\Upsilon\Xi+\Pi\Lambda}{\Pi\Gamma-\Theta\Xi(A_l/A_0)}, \tag{B.9}$$

where

$$\Gamma=1-\frac{1}{\overline{\rho}_l\overline{c}_l}\frac{\gamma\overline{p}_0}{\overline{M}_l\overline{c}_l}(\Psi-1), \tag{B.10}$$

$$\Lambda=1-\frac{1}{\overline{\rho}_0\overline{c}_0}\frac{\gamma\overline{p}_0}{\overline{M}_0\overline{c}_0}(\Psi-1), \tag{B.11}$$

$$\Xi=-1-\frac{1}{\overline{\rho}_0\overline{c}_0}\frac{\gamma\overline{p}_0}{\overline{M}_0\overline{c}_0}(\Psi-1), \tag{B.12}$$

$$\Psi=\left(\frac{\gamma-1}{\gamma}\right)\left[\frac{(1-\overline{M}_l^2)^{\gamma}-(1-\overline{M}_0^2)^{\gamma}}{(1-\overline{M}_l^2)^{\gamma-1}-(1-\overline{M}_0^2)^{\gamma-1}}\right], \tag{B.13}$$

$$\Theta=\frac{\gamma}{\gamma-1}\frac{\overline{p}_0}{\overline{\rho}_l\overline{c}_l}+\frac{\gamma}{\gamma-1}\overline{M}_0\overline{c}_0\left(1+\frac{\overline{\rho}_0\overline{c}_0}{\overline{\rho}_l\overline{c}_l}\overline{M}_0^2\right), \tag{B.14}$$

$$\Upsilon=-\frac{\gamma}{\gamma-1}\frac{\overline{p}_0}{\overline{\rho}_0\overline{c}_0}-\overline{M}_0\overline{c}_0\left[\frac{2\gamma-1}{\gamma-1}-\frac{1}{2}\overline{M}_0\left(\frac{A_l}{A_0}-1\right)(1+\overline{M}_0)\right], \tag{B.15}$$

$$\Pi=\frac{\gamma}{\gamma-1}\frac{\overline{p}_0}{\overline{\rho}_0\overline{c}_0}+\overline{M}_0\overline{c}_0\left[\frac{-1}{\gamma-1}-\frac{1}{2}\overline{M}_0\left(\frac{A_l}{A_0}-1\right)(1+\overline{M}_0)\right]. \tag{B.16}$$

Appendix C. Relative significance of acceleration of density inhomogeneities and steady heat communication mechanisms

Different authors [2,3,30] refer to either the acceleration of entropy disturbances or of density disturbances as a mechanism of sound generation. This appendix shows that reformulation of the source term D from Eq. (9) using density disturbances rather than entropy disturbances does not change any arguments put forward in this paper, i.e. sound generation by mean heat addition still dominates that of mean flow acceleration in the cases studied.

Eq. (9) can be rewritten in the following form:

$$D=D_{\mathrm{uhc}}+D^*_{\mathrm{shc}}+D^*_{\mathrm{mfa}}, \tag{C.1}$$

where

$$D^*_{\mathrm{shc}}=-\frac{\overline{q}A(\gamma-1)}{(\gamma)\overline{p}}(\overline{\rho}\overline{u}u'+p')\left(\frac{p'}{\overline{p}}+\frac{u'}{\overline{u}}\right)-\frac{A}{\overline{\rho}}\frac{\mathrm{d}\overline{\rho}}{\mathrm{d}x}p'\left(u'+\frac{\overline{u}p'}{\overline{\rho}\overline{c}^2}\right), \tag{C.2}$$

$$D^*_{\mathrm{mfa}}=-A\overline{u}\frac{\mathrm{d}\overline{u}}{\mathrm{d}x}\left(u'+\frac{\overline{u}p'}{\overline{\rho}\overline{c}^2}\right)\rho'. \tag{C.3}$$

This appendix presents an approximate analytical comparison of the source terms in Eq. (C.1) associated with the steady heat communication and mean flow acceleration at high frequencies. The results are applicable to low mean Mach numbers only. It is clear from the definition of D^*_{shc} and D^*_{mfa} that both of these terms are present in the flow at case A, while $D^*_{\mathrm{mfa}}=0$ throughout the flow in case B. Thus, the present analysis considers only case A.

Eqs. (1) and (2) can be linearised and combined to give

$$\frac{\partial p'}{\partial x}+\overline{\rho}\overline{u}\frac{\partial u'}{\partial x}+(\overline{\rho}u'+\overline{u}\rho')\frac{\mathrm{d}\overline{u}}{\mathrm{d}x}+\overline{\rho}\frac{\partial u'}{\partial t}=0. \tag{C.4}$$

By expressing density disturbances as entropy and pressure disturbances, see Section 1, Eq. (C.4) can be expressed as

$$\overline{\rho}\frac{\partial u'}{\partial t}+\frac{\partial p'}{\partial x}+\overline{\rho}\overline{u}\frac{\partial u'}{\partial x}-\left(\frac{\overline{\rho}\overline{u}}{c_p}s'-\overline{\rho}u'-\frac{\overline{M}}{\overline{c}}p'\right)\frac{\mathrm{d}\overline{u}}{\mathrm{d}x}=0. \tag{C.5}$$

C.1. High frequency limit

In the limit of infinite forcing frequency it has been shown in Ref. [13] that $|s'|\to 0$ in all cases studied here. Consider high forcing frequencies satisfying $\lambda_a \ll l$ where λ_a is the acoustic wavelength. It can be then argued that

$$\frac{\partial()}{\partial x} \simeq \frac{()}{\lambda_a} \simeq \frac{\omega}{\overline{c}}(), \quad \frac{\partial()}{\partial t} \simeq \omega(). \tag{C.6}$$

Further, for mean quantities

$$\frac{\mathrm{d}\overline{()}}{\mathrm{d}x} \simeq \frac{\Delta\overline{()}}{l}. \tag{C.7}$$

Substituting expressions (C.6) and (C.7) into (C.5) then results in

$$p' \simeq \frac{\overline{\rho c}[(\overline{M}+1)\omega+\Delta\overline{u}/l]}{\omega+\overline{M}\Delta\overline{u}/l}u' + \frac{\overline{\rho c u}\Delta u/c_p l}{\omega+\overline{M}\Delta\overline{u}/l}s'. \tag{C.8}$$

It is clear from relation (C.8) that the second term on the right hand side approaches zero at infinite frequency. In this limit relation (C.8) then simplifies at low Mach numbers to

$$\frac{p'}{\overline{p}} \simeq \gamma\overline{M}\frac{u'}{\overline{u}}. \tag{C.9}$$

Substitution of relation (C.9) into Eq. (C.3) reveals after some algebra that

$$D^*_{\mathrm{mfa}} \simeq -\frac{A\Delta\overline{u}\overline{\rho}}{l}\overline{M}u'^2. \tag{C.10}$$

Similarly, assuming a low Mach number mean flow, relation (C.2) becomes approximately

$$D^*_{\mathrm{shc}} \simeq -\gamma\frac{A\Delta\overline{\theta}}{\overline{\theta}l}\overline{\rho c}\overline{M}u'^2. \tag{C.11}$$

Further, for case A in the low Mach number limit, Eq. (2) indicates that the mean pressure can be assumed constant. Therefore it follows from the ideal gas law that $\overline{\rho}\,\mathrm{d}\overline{\rho}/\mathrm{d}\overline{x} \simeq -\overline{\theta}\,\mathrm{d}\overline{\theta}/\mathrm{d}\overline{x}$. Combining this with continuity of mass and using relation (C.6) gives

$$\frac{\Delta\overline{u}}{\overline{u}} \simeq \frac{\Delta\overline{\theta}}{\overline{\theta}}. \tag{C.12}$$

Applying relation (C.12) to relations (C.10) and (C.11) then results in

$$\left|\frac{D^*_{\mathrm{shc}}}{D^*_{\mathrm{mfa}}}\right| \simeq \frac{\gamma}{\overline{M}}, \tag{C.13}$$

which should hold at any given streamwise position in the inhomogeneous region.

Fig. 8 presents the spatially averaged value of the right hand side of relation (C.13), $1/l\int_0^l \gamma/\overline{M}\,\mathrm{d}x$. It also compares this theoretical result with $\Omega^* = 1/l\int_0^l \overline{D^*_{\mathrm{shc}}}/\overline{D^*_{\mathrm{mfa}}}\,\mathrm{d}x$, calculated by using the flow solver for the configuration in case A. The forcing frequency in each numerical simulation was chosen such that $\lambda_a/l < 0.2$ always. Further, entropy generation was

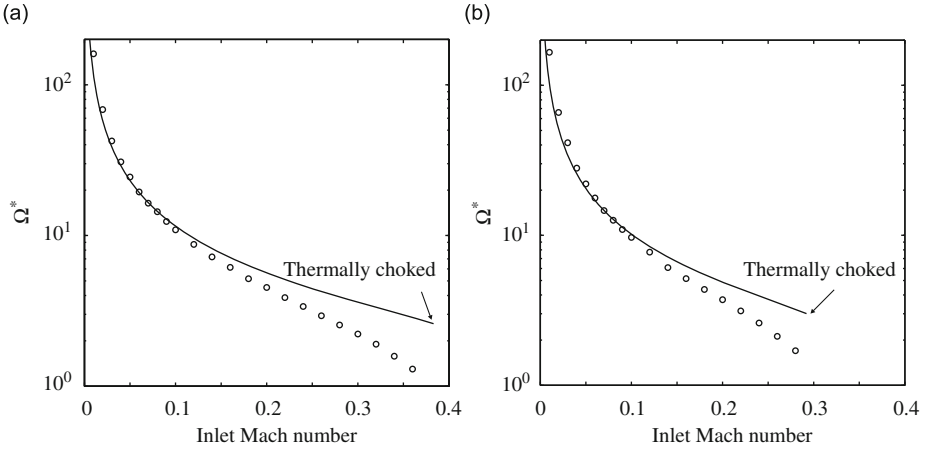

Fig. 8. Comparison between the analytical scaling and numerical simulation of Ω^* at high frequency and in case A for (a) stagnation temperature ratio of 2 and (b) stagnation temperature ratio of 3.

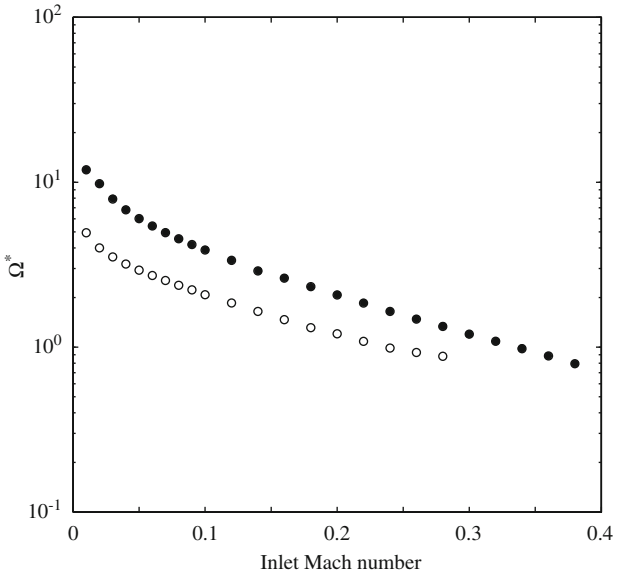

Fig. 9. Values of Ω^* for configuration in case A at low forcing frequency, calculated by numerical simulation. Dots and circles: stagnation temperature ratios of 2 and 3 respectively.

negligible at these frequencies. As can be seen in Fig. 8, theory and simulation are in very good agreement over the lower Mach number region, as was assumed in deriving the theoretical results.

It follows that at low Mach numbers and high forcing frequencies, the dominant source terms involve steady heat communication, and the effect of the source terms related to the acceleration of the mean flow is small. However, at close to sonic conditions the two sets of source terms have more comparable strength.

C.2. Low frequency limit

As $\omega \to 0$ the generation of entropy within the heat communicating region is significant [13]. Acceleration of these entropy disturbances then generates sound though the D^*_{mfa} source term and also greatly complicates the scaling analysis. Further, the numerical simulation takes longer to converge as $\omega \to 0$. Therefore, in this section we only present numerical results for Ω^* at frequencies such that $\lambda_c/l = 2$ always, where λ_c is the convective wavelength. It is noted that further decreases in the forcing frequency does not change the result significantly. Fig. 9 shows that in the low frequency limit the two sets of source terms D^*_{mfa} and D^*_{shc} have similar strength.

References

[1] L. Rayleigh, *Theory of Sound*, Macmillan, London, 1896.
[2] J.E. Ffowcs Williams, M.S. Howe, The generation of sound by density inhomogeneities in low Mach number nozzle flows, *Journal of Fluid Mechanics* 70 (1975) 605–622.
[3] M.S. Howe, Contributions to the theory of aerodynamic sound, with application to excess jet noise and the theory of flute, *Journal of Fluid Mechanics* 71 (1975) 625–673.
[4] M.S. Howe, *Acoustics of Fluid–Structure Interactions*, Cambridge University Press, New York, 1998.
[5] W.C. Strahle, Combustion noise, *Progress in Energy Combustion Science* 4 (1978) 157–176.
[6] S. Candel, D. Durox, S. Ducruix, A.L. Birbaud, N. Noiray, T. Schuller, Flame dynamics and combustion noise: progress and challenges, *International Journal of Aeroacoustics* 8 (2009) 1–56.
[7] N.A. Cumpsty, F.E. Marble, Core noise from gas turbine exhausts, *Journal of Sound and Vibration* 54 (1977) 297–309.
[8] F.E. Marble, S.M. Candel, Acoustic disturbance from gas non-uniformity convected through a nozzle, *Journal of Sound and Vibration* 55 (1977) 225–243.
[9] F. Bake, U. Michel, I. Roehle, Investigation of entropy noise in aero-engine combustor, *Journal of Engineering for Gas Turbines and Power* 129 (2007) 370–376.
[10] S. Kotake, On combustion noise related to chemical reactions, *Journal of Sound and Vibration* 42 (1975) 399–410.
[11] A.J. Kempton, Heat diffusion as a source of aerodynamic sound, *Journal of Fluid Mechanics* 78 (1976) 1–31.
[12] Y.L. Sinai, The generation of combustion noise by chemical inhomogeneities in steady, low-Mach-number duct flows, *Journal of Fluid Mechanics* 99 (1980) 383–397.
[13] N. Karimi, M.J. Brear, W.H. Moase, Acoustic and disturbance energy analysis of a flow with heat communication, *Journal of Fluid Mechanics* 597 (2008) 67–89.
[14] P.A. Hield, M.J. Brear, Comparison of open and choked premixed combustor exits during thermoacoustic limit cycle, *AIAA Journal* 46 (2008) 517–526.
[15] F. Nicoud, T. Poinsot, Thermoacoustic instabilities: should the Rayleigh criterion be extended to include entropy changes?, *Combustion and Flame* 142 (2005) 153–159
[16] T. Lieuwen, Theoretical investigation of unsteady flow interactions with a premixed planar flame, *Journal of Fluid Mechanics* 435 (2001) 289–303.
[17] A.P. Dowling, The calculation of thermoacoustic oscillation, *Journal of Sound and Vibration* 180 (1995) 557–581.

[18] P.A. Hield, M.J. Brear, S.H. Jin, Thermo-acoustic limit cycles in a premixed laboratory combustor with open and choked exits, *Combustion and Flame* 156 (2009) 1683–1697.
[19] N. Karimi, M.J. Brear, S.H. Jin, J.P. Monty, Linear and non-linear forced response of a conical, ducted, laminar premixed flame, *Combustion and Flame* 156 (2009) 2201–2212.
[20] G.J. Bloxsidge, A.P. Dowling, N. Hooper, P.J. Langhorne, Active control of reheat buzz, *AIAA Journal* 26 (1988) 783–790.
[21] C.L. Morfey, Acoustic energy in non-uniform flows, *Journal of Sound and Vibration* 14 (1971) 159–170.
[22] R.H. Cantrell, R.W. Hart, Acoustic energy in non-uniform flows, *Journal of Acoustical Society of America* 36 (1964) 697–706.
[23] C. Tam, J. Webb, Dispersion-relation-preserving finite difference scheme for computational acoustics, *Journal of Computational Physics* 107 (1993) 262–281.
[24] T. Poinsot, S. Lele, Boundary conditions for direct simulation of compressible viscous flows, *Journal of Computational Physics* 101 (1992) 104–429.
[25] C. Tam, H. Shen, *Direct computation of nonlinear acoustic pulse using high-order finite difference schemes*, AIAA Paper 93-4325, 1993.
[26] W.H. Moase, M.J. Brear, C. Manzie, The forced response of choked nozzles and supersonic diffusers, *Journal of Fluid Mechanics* 585 (2007) 281–304.
[27] S.M. Candel, Acoustic conservation principles and an application to plane and modal propagation and diffusers, *Journal of Sound and Vibration* 41 (1975) 207–232.
[28] A.P. Dowling, J.E. Ffowcs Williams, *Sound and Sources of Sound*, John Wiley, New York, 1983.
[29] P. Bala Subrahmanyam, R.I. Sujith, Acoustic Fields in inhomogeneous media: some exact harmonic solutions for variable area ducts and curvilinear geometries, *Acta Acoustica* 88 (2002) 837–841.
[30] C.L. Morfey, Amplification of aerodynamic noise by convected flow inhomogeneities, *Journal of Sound and Vibration* 31 (1973) 391–397.